Appl Phys B (2011) 105:685–688
DOI 10.1007/s00340-011-4760-4

Applied Physics B
Lasers and Optics

RAPID COMMUNICATION

Efficient and wavelength-tunable anti-Stokes frequency conversion with good beam quality in the fundamental mode of photonic crystal fiber

J.-H. Yuan · X.-Z. Sang · C.-X. Yu · L. Rao · Y. Han · G.-Y. Zhou · S.-G. Li · L.-T. Hou

Received: 14 March 2011 / Revised version: 28 June 2011 / Published online: 11 October 2011

Abstract Using the photonic crystal fiber (PCF) with the zero dispersion wavelength of 848 nm for the fundamental mode, the efficient anti-Stokes signal generations from 645 to 543 nm are realized by pumping in the normal dispersion region. When the pump average power increases from 200 to 500 mW, the output power of the anti-Stokes signal increases 8.46 times, the power ratio of the anti-Stokes signal at 543 nm to the residual pump is calculated as 22.6:1, and the conversion efficiency η in the experiment can be up to 46%. Moreover, good optical beam quality of the anti-Stokes signal can be achieved.

1 Introduction

Photonic crystal fibers (PCFs) [1, 2] have been shown to provide an attractive platform for realization of compact and efficient frequency conversion for microscopic and bioimaging applications [3, 4], as well as all optical nonlinear signal processing [5]. The nonlinear-optical frequency conversion and spectral transformation of laser radiation in PCFs [6–8] are often based on the sideband generation by four wave mixing (FWM). Since its first observation in PCFs [9], the FWM and phase-matching for frequency conversion in PCFs have been optimized in different ways [10]. To meet the phase-matching conditions, the pump should be in the vicinity of the zero dispersion wavelength of the guided-mode. PCFs allow the flexibility for the pump wavelength due to adjustable dispersion properties [11].

With the proper adjustment, the input pump energy can be easily coupled into the higher-order modes, and the efficient anti-Stokes signals can be generated by the phase-matched FWM. Akimov et al experimentally demonstrated the nonlinear-optical processes in the multimode PCFs, and achieved the up-frequency conversion of ultrashort laser pulses in the high-order modes of PCFs [12]. Hu et al. and we experimentally controlled the frequency transformations of femtosecond pulses in the second-order mode of PCFs [13, 14]. The anti-Stokes signal generation in the fundamental mode of PCF was elementarily investigated by us [15]. Compared with the higher-order modes, it is easier to couple into the fundamental mode of PCFs for the input pump pulse, and the output optical beam has better quality. However, it's difficult to achieve the phase-matching condition for the fundamental mode in the general multimode PCF with the regular short pulse source, since its zero dispersion wavelength often lies at the longer wavelength relative to the high-order modes. In this paper, the phased-matched FWM processes of femtosecond pulses in the fundamental mode of PCF designed and fabricated in our lab are presented. By pumping in the normal dispersion region, the anti-Stokes signals from 645 to 543 nm can be efficiently generated as the input average power increases from 200 to 500 mW. The maximum ratio of anti-Stokes signal at 543 nm to the residual pump component is calculated as 22.6:1, and the maximum conversion efficiency of 46% in the experiment is achieved. The output optical beam of anti-Stokes signal is with good quality.

J.-H. Yuan (✉) · X.-Z. Sang · C.-X. Yu · L. Rao
State Key Laboratory of Information Photonics and Optical Communications, Beijing University of Posts and Telecommunications, P.O. Box 163#, BUPT, 100876 Beijing, China
e-mail: yuanjinhui81@163.com
Fax: +86-106-2281162

Y. Han · G.-Y. Zhou · S.-G. Li · L.-T. Hou
Institute of Infrared Optical Fibers and Sensors, Physics Department, Yanshan University, 066004, Qinhuangdao, China

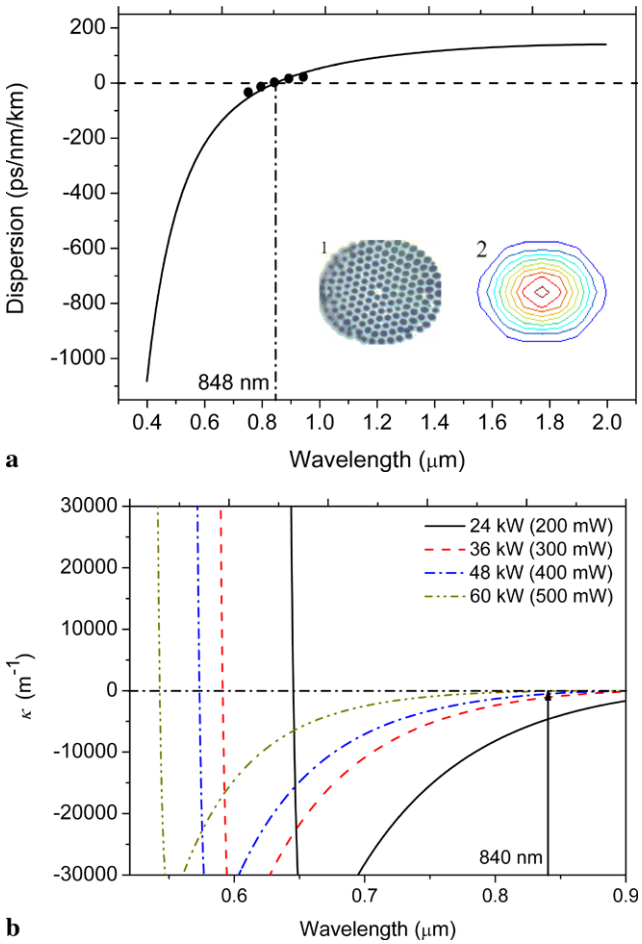

Fig. 1 (**a**) Group-velocity dispersion calculated as a function of radiation wavelength for the fundamental mode, the solid-dot indicating the measured values by the pulse time-delay method, the *insets 1* and *2* showing the cross-section of PCF and the simulation result for the transverse field intensity distribution of the fundamental mode, the vertical dash line corresponding to the zero dispersion wavelength of 848 nm. (**b**) The phase-mismatching parameter κ in the fundamental mode as a function of radiation wavelength under different input power at the short wavelengths, the vertical arrow line corresponding to the pump working wavelength of 840 nm

2 The PCF properties and experiment

The Multi-pole method (MPM) is used to analyze the properties of waveguide mode in PCF. Figure 1(a) is the group velocity dispersion of fundamental mode calculated as a function of radiation wavelength, where the zero dispersion wavelength of 848 nm agrees well with the measured result by the pulse time-delay method, and the material dispersion is calculated from the Sellmeyer equation. The cross-section structure of PCF used is shown in the inset 1 of Fig. 1(a). To choose the appropriate PCF parameters, the frequency relations between the signals (the Stokes and anti-Stokes signals) and pump are described as $\omega_{s,a} = \omega_p \mp \sqrt{-\beta^{(2)}(\omega_p)/[12\beta^{(4)}(\omega_p)]}$ by expansion of $\beta(\omega)$ up to

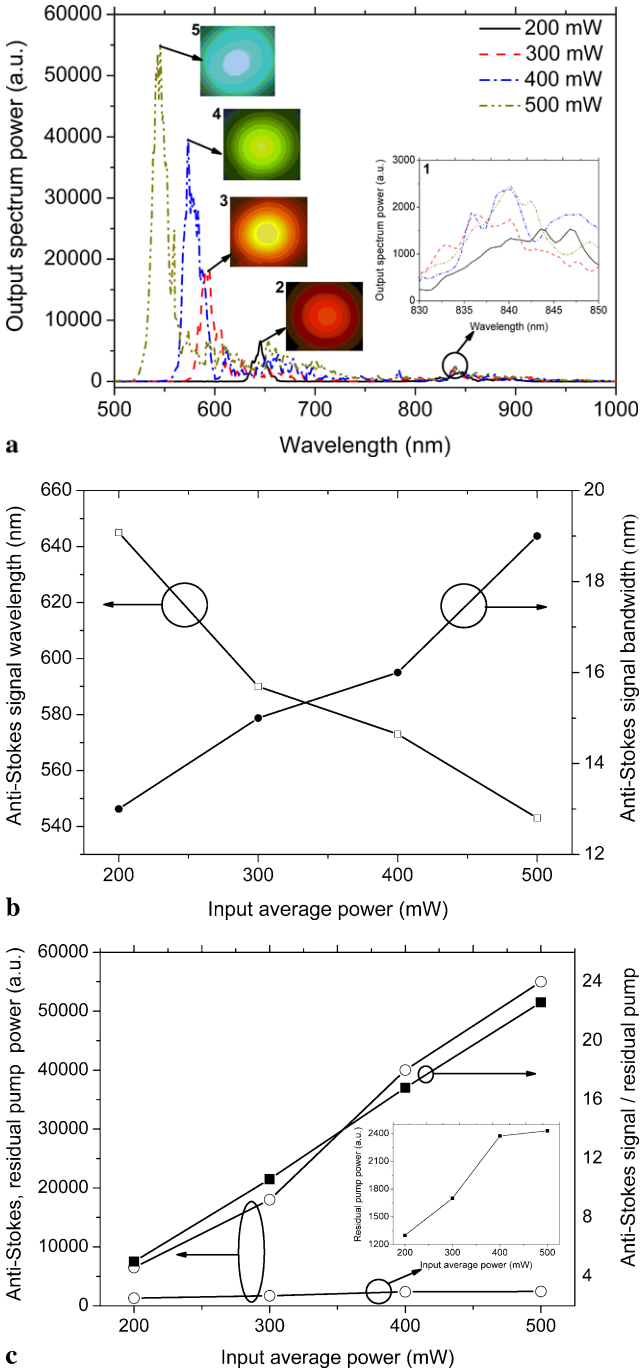

Fig. 2 (**a**) The output spectra with the input average power increasing from 200 to 500 mW. The *inset 1* shows the amplified output spectra of residual pump component, and the *insets 2* to *5* correspond to the output far fields of different signal (*red*, *orange-yellow*, *yellow-green*, and *weak-green light*). (**b**) The anti-Stokes signal wavelength (*square solid line*) and bandwidth (*circle solid line*) as a function of input average power. (**c**) The ant-Stokes signal and residual pump power (*circle solid lines*) and the ratio of anti-Stokes signal and residual pump (*square solid line*) as a function of input average power. The *inset* shows the residual pump power (*square solid line*)

the fifth order around ω_p with the nonlinear term neglected, where $\beta^{(n)} = \partial^n \beta(\omega)/\partial\omega^n$ and the signs of $\beta^{(2)}(\omega_p)$ and $\beta^{(4)}(\omega_p)$ should be different for phase-matching to occur. The silica PCF is specially designed in order to satisfy the phase-matching condition at the specific wavelength, and the structure parameters are as follows: the relative air-hole size is 0.86, and the core diameter is 2.8 μm. Inset 2 of Fig. 1(a) shows the simulation result for the transverse field intensity distribution of the fundamental mode. The degenerate four-wave mixing, which involves a pump and a Stokes wave at frequency ω_p and ω_s to produce a signal wave at $2\omega_p - \omega_s$, can be used for the anti-Stokes frequency conversion of the ultra-short laser pulse. When a strong pump pulse at ω_p is launched into the fiber, a Stokes signal with downshifted frequency ω_s and an anti-Stokes signal with upshifted frequency ω_a are simultaneously generated. To achieve high energy transfer from the pump to the signal under different input power values, the phase-matching condition $\kappa = \beta(\omega_s) + \beta(\omega_a) - 2\beta(\omega_p) + 2n_2\omega_p P_p/(cA_{eff}) = 0$ should be satisfied, where $\beta(\omega_p)$, $\beta(\omega_a)$, and $\beta(\omega_s)$ correspond to the propagation constants of pump, anti-Stokes signal, and Stokes signal, P_p is the pump peak power, n_2 is the nonlinear refractive index, c is the light velocity in the vacuum, and A_{eff} is the effective mode field area. The phase-mismatching case of the fundamental mode at the short wavelength is presented in Fig. 1(b) when the pump works at 840 nm and the peak power increases from 24 to 60 kW (corresponding to the average powers of 200 to 500 mW). The phase-mismatching parameter κ reaches zero at the wavelengths of 645 nm, 590 nm, 573 nm, and 543 nm.

In the experiment, the light source is a Kerr Lens Mode-locking (KLM) Ti:sapphire ultrafast laser at 840 nm, which emits a pulse train with FWHM of 120 fs at the repetition rate of 76 MHz. By changing the distance between the input tip of the fiber and the lens to exactly adjust the angle between the input beam and the fiber axis, the fundamental mode can be selectively excited. The pump energy is coupled into the PCF span of 50 cm length, and the coupling efficiency is 65%. The transmission loss is measured to be 5.8 dB/m at 840 nm with the cut-back method. The output far fields are observed by CCD. The spectral properties of the output radiation are monitored by an optical spectrum analyzer (OSA) with the measurement scope from 200 to 1100 nm and a resolution of 0.025 nm.

3 Results and discussion

At the initial stage of nonlinear process, because the pump wavelength approaches the zero dispersion wavelength of PCF, the self-phase modulation (SPM) plays a main role. Frequency components of the input pulse serve as a pump for phase-matched FWM, deplete the radiation spectrum around the zero dispersion wavelength, and transfer the radiation energy to the normal and anomalous dispersion regions, as shown in the inset 1 of Fig. 2(a). Moreover, the FWM effect is more remarkable due to less κ, and the anti-Stokes signals are efficiently generated within the wavelength range of 645 to 543 nm, as shown in Fig. 2(a). The experimental results agree well with the theoretical results in Fig. 1(b). The insets 2 to 5 show the observed output far field modes at different signal wavelengths (red, orange-yellow, yellow-green, and weak green light), corresponding to the inset 2 of Fig. 1(a). In Fig. 2(b), with the input average power increasing, the central wavelengths and bandwidths of the anti-Stokes signals change noticeably whereas nearly inverse changing trends. The wide wavelength-tunable range (>100 nm) and broadband visible wavelength (~19 nm) are achieved. As shown in Fig. 2(c), the output power of the anti-Stokes signal increases 8.46 times as the input average power increases from 200 to 500 mW. The output power ratio of anti-Stokes signal at 543 nm and the residual pump component (as shown in the inset of Fig. 2(c)) can be up to 22.6:1. The anti-Stokes radiation is above 85% of the total output power, calculated from the Manley–Rowe relations of photon conservation.

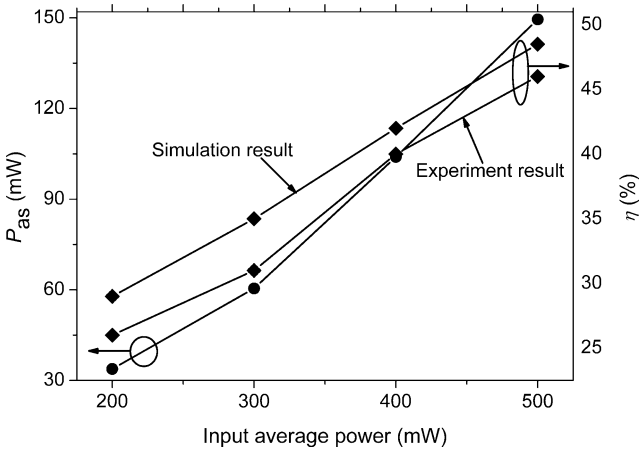

Fig. 3 The measured output anti-Stokes signal power P_{as} (*circle solid line*) and conversion efficiency η (*square solid lines*) as a function of the input average power

The conversion efficiency (η) of the degenerate FWM can be described by the power ratio of the output anti-Stokes signal P_{as} and incident pump $P_{p0}(P_{as}/P_{p0})$. In Fig. 3, with different input average powers, the measured P_{as} are 33.8 mW, 60.5 mW, 104 mW, and 149.5 mW. For the determinate coupling efficiency (65%), the maximal η in the experiment is estimated as 46%. Considering the depletion of pump, a constant value for nonlinearity, a single effective overlap integral, and no loss, the values of η can be theoretically calculated [16–18]. The maximal η of 48.5% corresponds to the signal generation at 543 nm. The tiny discrepancy between the experimental and theoretical result

may arise from the pulse walk-off between the pump and anti-Stokes wave due to large wavelength separation, and the coupling and scattering loss of the high-order modes because of large index contrast between the core and cladding region. The FWHM of initial pump pulse of 120 fs is broadened to 650 fs because of the dispersion and nonlinear effect, and the estimated width of the anti-Stokes signal pulse at 543 nm is 55 fs.

Moreover, as seen from Fig. 2(a), the output powers of the trivial components at longer wavelengths, resulting from part of pump energy coupling into other polarization state of the fundamental mode and the Raman cascade effect, and residual pump components are lower. It is possible that the total energy of the Stokes frequency components corresponding to the phase-matching conditions at long wavelengths is entirely depleted at the output of fiber due to tens or hundreds of dB/m transmission loss. Thus, the output signal interference can be greatly depressed, and good optical beam quality of the anti-Stokes signal can be obtained, as shown in the insets 2 to 5 of Fig. 2(a).

4 Conclusion

In summary, the efficient and wavelength-tunable anti-Stokes frequency conversion is achieved with the phase-matched FWM in the fundamental mode of PCF pumped in the normal dispersion region. The related nonlinear process is demonstrated. In addition, good optical beam quality of the anti-Stokes signal is obtained.

Acknowledgements This work is partly supported by the National Key Basic Research Special Foundation (2010CB327605 and 2010CB328300), the Fundamental Research Funds for the Central Universities (2011RC0309), the key grant of Chinese Ministry of Education (No. 109015), the discipline Co-construction Project of Beijing Municipal Commission of Education (YB20081001301), and the Specialized Research Fund for the Doctoral Program of Beijing University of Posts and Telecommunications (CX201023).

References

1. P.St.J. Russell, Science **299**, 358 (2003)
2. J.C. Knight, Nature (London) **424**, 847 (2003)
3. S.O. Konorov, D.A. Akimov, E.E. Serebryannikov, A.A. Voronin, M.V. Alfimov, A.M. Zheltikov, Phys. Rev. E **70**, 057601 (2004)
4. A.A. Ivanov, A.A. Podshivalov, A.M. Zheltikov, Opt. Lett. **31**, 3318 (2006)
5. X. Sang, P.K. Chu, C. Yu, Opt. Quantum Electron. **37**, 965 (2005)
6. A.B. Fedotov, I. Bugar, D.A. Sidorov-Biryukov, E.E. Serebryannikov, D. Chorvat Jr., M. Scalora, D. Chorvat, A.M. Zheltikov, Appl. Phys. B **77**, 313 (2003)
7. L. Tartara, I. Cristiani, V. Degiorgio, Appl. Phys. B **77**, 307 (2003)
8. E.E. Serebryannikov, A.M. Zheltikov, N. Ishii, C.Y. Teisset, S. Köhler, T. Fuji, T. Metzger, F. Krausz, A. Baltuška, Appl. Phys. B **81**, 585 (2005)
9. J.E. Sharping, M. Fiorentino, A. Coker, P. Kumar, R.S. Windeler, Opt. Lett. **26**, 1048 (2001)
10. S. Asimakis, P. Petropoulos, F. Poletti, J.Y.Y. Leong, R.C. Moore, K.E. Frampton, X. Feng, W.H. Loh, D.J. Richardson, Opt. Express **15**, 596 (2007)
11. A.B. Fedotov, E.E. Serebryannikov, A.A. Ivanov, L.A. Mel'nikov, A.V. Shcherbakov, D.A. Sidorov-Biryukov, Ch.-K. Sun, M.V. Alfimov, A.M. Zheltikov, Laser Phys. Lett. **3**, 301 (2006)
12. D.A. Akimov, E.E. Serebryannikov, A.M. Zheltikov, M. Schmitt, R. Maksimenka, W. Kiefer, K.V. Dukel'skii, V.S. Shevandin, Yu.N. Kondrat'ev, Opt. Lett. **28**, 1948 (2003)
13. M.L. Hu, C.Y. Wang, Y.J. Song, Y.F. Li, L. Chai, Opt. Express **14**, 1189 (2006)
14. J.H. Yuan, X.Z. Sang, C.X. Yu, X.J. Xin, G.Y. Zhou, S.G. Li, L.T. Hou, Appl. Phys. B **104**, 117 (2011)
15. J.H. Yuan, X.Z. Sang, C.X. Yu, S.G. Li, G.Y. Zhou, L.T. Hou, IEEE J. Quantum Electron. **46**, 728 (2010)
16. A.V. Husakou, J. Herrmann, Appl. Phys. Lett. **83**, 3867 (2003)
17. G.P. Agrawal, *Nonlinear Fiber Optics* (Academic, New York, 1994)
18. Y.Q. Xu, S.G. Murdoch, R. Leonhardt, J.D. Harvey, Opt. Lett. **33**, 1351 (2008)